Analytical Formulation for the micro-Doppler Spectrum for Rotating Targets in the Near-Field

Jean Léger[1], Thomas Pairon[1], Christophe Craeye[1]
[1]ICTEAM : Université Catholique de Louvain, 1348, Louvain-la-Neuve, Belgique

***Abstract*—The analysis of the Doppler signal returned by rotating targets is of great interest in the framework of target recognition and equipment monitoring. An analytical expression of such a signal already exists for the far-field case, based on the Jacobi-Anger expansion. An extension of this analytical expression is proposed for the near-field case. The solution involves a closed-form expression of each harmonic complex coefficient. An error analysis is carried out.**

***Index Terms*—Jacobi-Anger expansion, Bessel functions, rotating targets, micro-Doppler, near-field, radar cross section.**

I. Introduction

When a target moves along the radar line of sight with a constant speed, the carrier frequency of the return signal is shifted. This is known as the Doppler phenomenon. However, many radar targets are composed of several parts moving at different speeds or are moving with a time-varying radial speed. This gives rise to a wide Doppler spectral content called the micro-Doppler spectrum [1]. Since this micro-Doppler spectrum is specific to the precise motion and the geometry of the target, it can be used as a discriminative signature in a classification framework.

In particular, vibrating and rotating targets have been modelled and simulated in order to show the frequency modulation that they introduce [1]. For vibrations, an analytical derivation allows us to express the return signal $s(t)$ by means of Bessel functions of the first kind. In this case, the micro-Doppler spectrum consists of a limited number of spectral lines pairs around 0 Hz. This can be done for rotations as well, provided that the far-field assumption is satisfied (i.e. a target located at a distance R from the radar with $R \geq 2D^2/\lambda$, where D is the maximal size of the target and λ corresponds to the wavelength). In [2] and [3], the Jacobi-Anger expansion is used in order to express the micro motion signal of a point located on a rotating car wheel. In [4] and [5], such approaches are respectively used in order to obtain the return signal from a wind-turbine and an helicopter. In [6], these functions are used in the framework of ISAR imaging of targets with rotating parts. Other works also consider rotating targets without referring to the Jacobi-Anger expansion [7], [8].

However, in several recent applications, the far-field assumption is not satisfied. In [9], it is proposed to place the radar very close to the turbine in order to extract information about the structural health status of wind turbines. In [10], the radar cross section and the received signal are analysed considering a forward scattering radar in the near-field. A Taylor series expansion of the return signal phase is used in [11] for RCS computations in the near-field, in the monostatic case. In road monitoring applications, the Doppler signature of a rotating wheel could be used as a classification criterion. However, for a radar operating at 24 GHz, the far-field condition requires a minimal distance of approximately 20 meters between target and radar, which may not be met in many applications.

This paper is organized as follows. In Section II, the analytical expression of the Doppler spectrum of a rotating target is derived. This is carried out using Taylor series expansions of the phase term of the radar return signal, combined with the integral representation of Bessel functions. The derivation is firstly provided in the far-field region (Section II-A). Then, an extension of the analytical expression is proposed in order to take the near-field effects into account (Section II-B). An error analysis of the proposed analytical closed-form is studied for different geometries, frequencies and distances from the radar in Section III. Finally, Section IV provides concluding remarks.

II. Mathematical description

Let us consider a monostatic coherent radar located at P as shown in Fig. 1. The complex envelope of the signal $s(\theta)$ scattered by a rotating point target can be written as

$$s(\theta) = \frac{A}{R^2(\theta)} e^{-2jkR(\theta)}, \tag{1}$$

where A models the signal amplitude (RCS, losses etc.), k is the wavenumber, θ is the angular position of the point scatterer and $R(\theta)$ is the distance between the radar and the point scatterer. The rotation speed Ω is assumed to be constant, hence $\theta = \Omega t$. Referring to Fig. 1, the distance $R(\theta)$ can be written as

$$R(\theta) = R_0 \sqrt{1 + \frac{a^2}{R_0^2} + 2\frac{a}{R_0}\cos(\theta)}, \tag{2}$$

where a is the rotation radius and R_0 is the distance between the radar and the rotation center. Equation (2) can be expanded into a Taylor series as

$$R(\theta) = R_0\sqrt{1+\epsilon_1} = R_0\left(1 + \frac{\epsilon_1}{2} - \frac{\epsilon_1^2}{8} + \mathcal{O}(\epsilon_1^3)\right), \tag{3}$$

with

$$\epsilon_1 = a^2/R_0^2 + 2a/R_0\cos(\theta). \tag{4}$$

The goal of this paper is to derive the analytical expression of the micro-Doppler spectrum of (1) (i.e. the Fourier transform of $s(\theta)$ over one complete rotation). The method consists in developing (3) to different successive orders and using the integral representation of Bessel functions. For the sake of simplicity, the $R(\theta)$ factor present in the amplitude is approximated by a constant value such that $R(\theta) \approx R_0$.

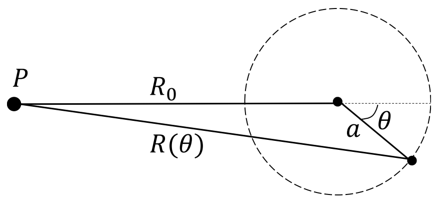

Fig. 1: Geometrical description of the problem.

A. Far-field conditions

When limiting (3) to the first order, the distance $R(\theta)$ becomes

$$R(\theta) \approx R_0 + \frac{a^2}{2R_0} + a\cos(\theta). \tag{5}$$

Up to the constant phase term $a^2/2R_0$, (5) is equal to the classical form of $R(\theta)$ under the far-field approximation. Substituting (5) into (1), the return signal $s(\theta)$ can be approximated as

$$s_1(\theta) = A' e^{-2jka\cos(\theta)}, \tag{6}$$

where $A' = A/R_0^2 \ \exp\left(-jk(2R_0 + a^2/R_0)\right)$. Since $s_1(\theta)$ is periodic, it can be represented as a Fourier series as [12]

$$s_1(\theta) = \sum_{n=-\infty}^{\infty} S_1[n] e^{jn\theta}, \tag{7}$$

where the $S_1[n]$ coefficients are obtained as

$$S_1[n] \quad = \quad \frac{A'}{2\pi}\int_0^{2\pi} e^{-2jka\cos(\theta)} \ e^{-jn\theta} \ \mathrm{d}\theta. \tag{8}$$

In order to compute (8) analytically, the integral representation of Bessel functions can be used (which is equivalent to use the Jacobi-Anger formula [13]) and yields

$$S_1[n] \quad = \quad A' j^n J_n(-2ka), \tag{9}$$

where J_n is the n-th Bessel function of the first kind. Result (9) is equivalent to formulas found in [4]. As stated above, this shows that the micro-Doppler spectrum consists of a limited number of spectral lines pairs around 0 Hz since $J_{-n}(z) = (-1)^n J_n(z)$ and $J_n(z)$ tends to zero for a large n. More precisely, the micro-Doppler spectrum bandwidth (in the positive frequencies) BW can be obtained as a function of the rotation speed Ω as

$$BW \quad = \quad \frac{2a\Omega}{\lambda}, \tag{10}$$

where λ is the wavelength. Hence, the maximum number of spectral lines (in the positive frequencies) n_{max} reaches about $2a/\lambda$.

B. Near-field conditions

The result (9) holds in the far-field region. In this section, the near-field effects are taken into account by expanding (3) to the second order. The return signal $s_2(\theta)$ obtained with this improved approximation is written as a function of two parameters having a physical meaning.

The parameter δ (called far-field parameter in this work, also used in [14]) is proportional to the ratio between the far-field limit $2(2a)^2/\lambda$ and the distance R_0,

$$\delta \quad = \quad \frac{ka^2}{R_0}. \tag{11}$$

Hence, the far-field approximation ($R_0 \geq 2(2a^2)/\lambda$) is satisfied when $\delta < \pi/4$.

The second parameter η (called dimensions ratio in this work) allows us to link the characteristic size of the target a and the distance R_0 between the radar and the rotation center, that is

$$\eta = \frac{R_0}{a}. \tag{12}$$

Using parameters δ and η with approximation (3), the return signal $s_2(\theta)$ is expressed as

$$s_2(\theta) = A'' e^{j\gamma\cos(\theta)} e^{j\delta\cos(2\theta)/2}, \tag{13}$$

where $\gamma = -\delta(2\eta - 1/\eta)$ and A'' is a constant complex number such that $A'' = A/R_0^2 \exp\left(-j\delta(2\eta^2 + 0.5 - 0.25/\eta^2)\right)$.

Finding a Fourier series for (13) is not immediate. Therefore, a second Taylor series expansion is carried out. Writing $\epsilon_2 = j\cos(2\theta)\delta/2$, the following expansion is used

$$\exp(\epsilon_2) \quad = \quad 1 + \epsilon_2 + \frac{\epsilon_2^2}{2} + \mathcal{O}(\epsilon^3). \tag{14}$$

Moreover, one can also show that

$$\epsilon_2 \quad = \quad j\frac{\delta}{4}\left(e^{j2\theta} + e^{-j2\theta}\right), \tag{15}$$

$$\frac{\epsilon_2^2}{2} \quad = \quad -\frac{\delta^2}{16}\left(1 + \frac{1}{2}\left(e^{j4\theta} + e^{-j4\theta}\right)\right). \tag{16}$$

The complex exponentials in (15), (16) lead to a closed-form Fourier series approximation of (13) through integrals similar to (8). For clarity, the notation $s_{p,q}(\theta)$ is introduced for the approximation of $s(\theta)$ where p and q respectively stand for the order of the Taylor expansions given in (3) and (14). Using (13) to (16), the Fourier series are

$$\begin{aligned} S_{2,1}[n] \quad = \quad & \frac{A''}{2\pi}\int_0^{2\pi} e^{j\gamma\cos(\theta)} \left(e^{-jn\theta} + j\frac{\delta}{4}e^{-j(n-2)\theta} \right. \\ & \left. + j\frac{\delta}{4}e^{-j(n+2)\theta}\right) \mathrm{d}\theta, \end{aligned} \tag{17}$$

$$\begin{aligned} S_{2,2}[n] \quad = \quad & \frac{A''}{2\pi}\int_0^{2\pi} e^{j\gamma\cos(\theta)} \left(\left(1 - \delta^2/16\right) e^{-jn\theta} \right. \\ & + j\frac{\delta}{4}e^{-j(n-2)\theta} + j\frac{\delta}{4}e^{-j(n+2)\theta} \\ & \left. - \frac{\delta^2}{32}e^{-j(n-4)\theta} - \frac{\delta^2}{32}e^{-j(n+4)\theta} \right) \mathrm{d}\theta. \end{aligned} \tag{18}$$

Using the Jacobi-Anger expansion, (17) and (18) become

$$\begin{aligned} S_{2,1}[n] &= A'' \bigg(j^n J_n(\gamma) + j\frac{\delta}{4} \left(j^{n-2} J_{n-2}(\gamma) \right. \\ &\quad + \left. \left. j^{n+2} J_{n+2}(\gamma) \right) \right), \end{aligned} \tag{19}$$

$$\begin{aligned} S_{2,2}[n] &= A'' \left(\left(1 - \delta^2/16\right) j^n J_n(\gamma) \right. \\ &\quad + j\frac{\delta}{4} \left(j^{n-2} J_{n-2}(\gamma) + j^{n+2} J_{n+2}(\gamma) \right) \\ &\quad \left. - \frac{\delta^2}{32} \left(j^{n-4} J_{n-4}(\gamma) + j^{n+4} J_{n+4}(\gamma) \right) \right). \end{aligned} \tag{20}$$

As observed for (9), the micro-Doppler spectra defined by (19) and (20) consist of a limited number of spectral lines pairs around 0 Hz. The approximation $s_{2,q}(\theta)$ of the temporal return signal $s(\theta)$ can be obtained with

$$s_{2,q}(\theta) = \sum_{n=-\infty}^{\infty} S_{2,q}[n] e^{jn\theta}. \tag{21}$$

III. Results

From (7) and (21), it can be observed that the approximations of $s(\theta)$ depend only on the far-field parameter δ and the dimensions ratio η given in (11) and (12), even if the discussed scenario has three key parameters: R_0, a and λ.

In Figs. 2(a) to 2(d), the relative error made with the approximations is provided as a function of the far-field parameter δ for several values taken by the dimensions ratio, i.e. $\eta = 1, 8, 64, 512$. The following metric is used in order to compute the relative energy error e_{rel}

$$e_{\text{rel}} = \frac{\int_0^{2\pi} \left| s(\theta) - s_{approx}(\theta) \right|^2 \mathrm{d}\theta}{\int_0^{2\pi} \left| s(\theta) \right|^2 \mathrm{d}\theta}, \tag{22}$$

where $s_{approx}(\theta)$ is $s_1(\theta)$, $s_2(\theta)$, $s_{2,1}(\theta)$ or $s_{2,2}(\theta)$. Several observations can be made based on Figs. 2(a) to 2(d).

1) For a fixed geometry up to a scaling factor (a constant dimensions ratio η), the error increases with the far-field parameter δ (or decreases with λ).
2) The error made with $s_1(\theta)$ does not depend on the dimensions ratio η on the studied ranges of the parameters δ and η. At $\delta = \pi/4$ (i.e. the limit of the far-field region), the relative energy error is higher than 0.1, which is already a large error.
3) Working with the second order Taylor expansion of the square root allows us to reduce the error provided that the dimensions ratio η is not too small, as shown by $s_2(\theta)$.
4) In practice, the Taylor expansion (14) of the exponential limits the accuracy of the approximation as shown in Figs. 2(c) and 2(d). Hence, $s_2(\theta)$ provides a lower bound on the error, which can be reached by adding orders in the second Taylor expansion (at the expense of more complex analytical expressions for $S_{2,q}[n]$).

It has also been observed that the error made with $s_1(\theta)$ mostly affects the phase of the spectrum $S_1[n]$. Indeed, the magnitude of $S_1[n]$ is even more accurate than the magnitude of $S_2[n]$.

Finally, the errors $e_{\text{rel},1}(\delta,\eta)$ and $e_{\text{rel},2}(\delta,\eta)$ respectively made with $s_1(\theta)$ and $s_2(\theta)$ can be written as follows based on a curve-fitting on Figs. 2(a) to 2(d):

$$e_{\text{rel},1}(\delta,\eta) = 0.1939 \left(\frac{4\delta}{\pi}\right)^2, \tag{23}$$

$$e_{\text{rel},2}(\delta,\eta) = 0.2107\ \eta^{-2} \left(\frac{4\delta}{\pi}\right)^2. \tag{24}$$

IV. Conclusion

Under the far-field approximation, the micro-Doppler spectrum associated to a rotating target can be expressed in closed-form via the Jacobi-Anger relation. However, in the near-field region (and even at the limit of the far-field region), the energy of the error using this expression exceeds one tenth of the received signal energy.

Hence, an extension of the existing analytical expression has been proposed using two successive Taylor series expansions on the return signal phase term. In order to capture the near-field effects, the first Taylor series is expanded up to the second order. The second expansion allows us to write the return signal as the sum of Bessel functions of the first kind. The proposed method gives a significant accuracy improvement in the different studied configurations, typically by 2 to 4 orders of magnitude at the far-field limit for distances ranging for 8 to 500 times the radius of rotation.

The development is limited to point-like scatterers. Further investigation is necessary to extend this analytical method to more complex structures (such as car wheels, UAV blades, windturbines, etc.) and to use it in classification, surveillance or maintenance applications. Further research could also focus on the performance improvement reached when the signal amplitude variation is taken into account with an appropriate series expansion.

References

[1] V. Chen *et al.*, "Micro-doppler effect in radar: phenomenon, model, and simulation study," *IEEE Trans. Aerosp. Electron. Syst.*, vol. 42, no. 1, pp. 2-21, 2006.

[2] Y. Li *et al.*, "Hierarchical classification of moving vehicles based on empirical mode decomposition of micro-Doppler signatures," *IEEE Trans. Geosci. Remote Sensing*, vol. 51, no. 5, pp. 3001-3013, 2013.

[3] L. Du *et al.*, "Micro-Doppler feature extraction based on time-frequency spectrogram for ground moving targets classification with low-resolution radar," *IEEE Sensors J.*, vol. 16, no. 10, pp. 3756-3763, 2016.

[4] O. Krasnov and A. Yarovoy, "Radar micro-Doppler of wind turbines: simulation and analysis using rotating linear wire structures," *Int. J. Microw. Wireless Technol.*, vol. 7, no. 3-4, pp. 459-467, 2015.

[5] T. Thayaparan *et al.*, "Analysis of radar micro-Doppler signatures from experimental helicopter and human data," *IET Radar, Sonar and Navigation*, vol. 1, no. 4, p. 289, 2007.

[6] X. Bai *et al.*, "Imaging of micromotion targets with rotating parts based on empirical-mode decomposition," *IEEE Trans. Geosci. Remote Sensing*, vol. 46, no. 11, pp. 3514-3523, 2008.

[7] A. Cilliers and W. Nel, "Helicopter parameter extraction using joint time-frequency and tomographic techniques," *2008 Int. Conf. on Radar*, Adelaide, Australia, Sept. 2-5 2008.

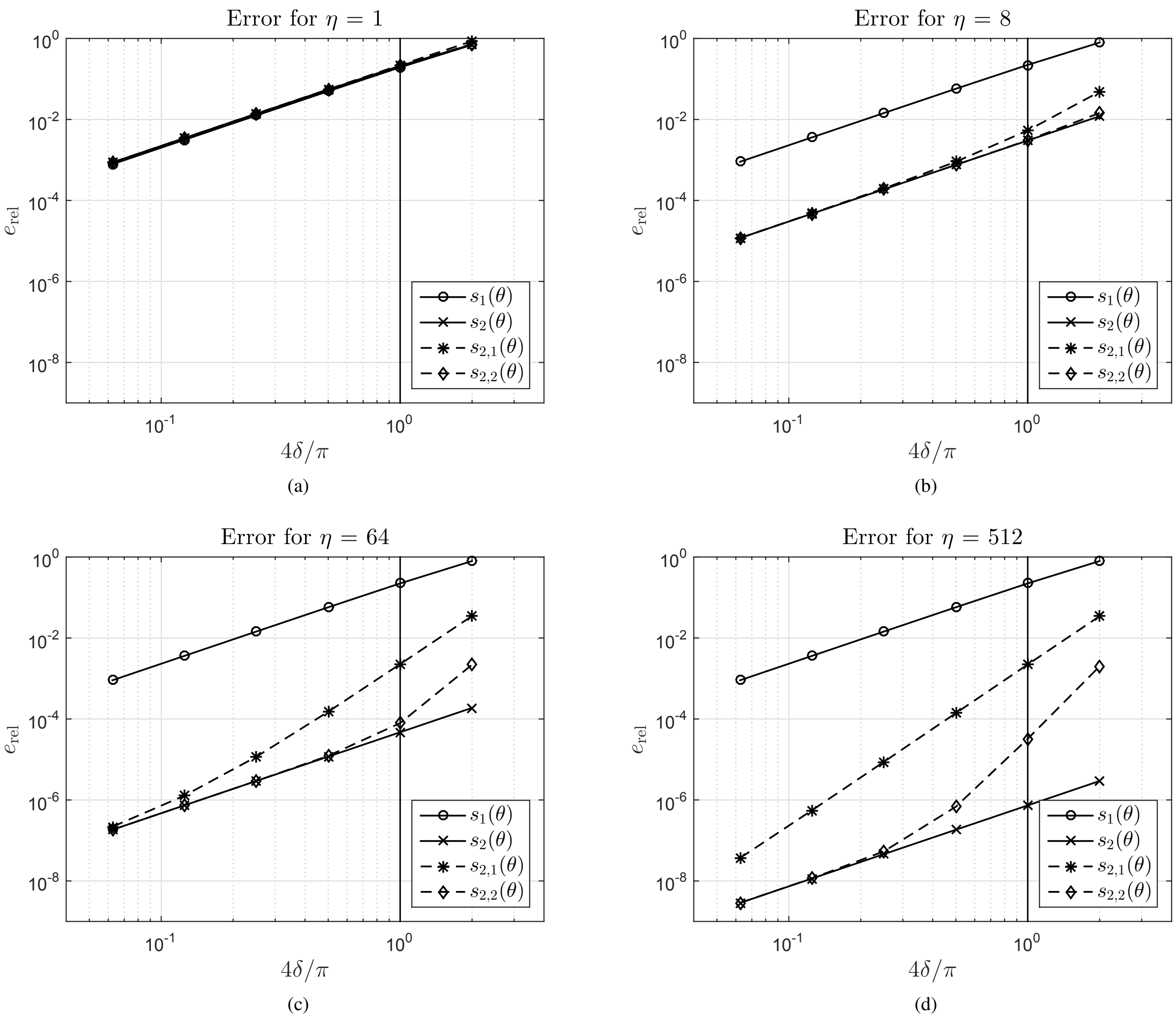

Fig. 2: Error defined by (22) versus δ for different values of η: (a) $\eta = 1$, (b) $\eta = 8$, (c) $\eta = 64$, (d) $\eta = 512$. Vertical line : far-field limit.

[8] P. Molchanov *et al.* "Classification of small UAVs and birds by micro-Doppler signatures," *Int. J. Microw. Wireless Technol.*, vol. 6, no. 3-4, pp. 435-444, 2014.

[9] M. Crespo-Ballesteros and M. Antoniou, "Wind turbine radar signature analysis in the near-field," *2014 Int. Radar Conf.*, 2014.

[10] M. Falconi *et al.*, "Analysis of canonical targets in near-field for forward scatter radar applications," *Proceedings of the 12th European Radar Conference*, 2015.

[11] P. Pouliguen *et al.*, "Analytical formulae for radar cross section of flat plates in near-field and normal incidence," *Progress In Electromagnetics Research B*, vol. 9, pp. 263-279, 2008.

[12] S. Haykin and B. Van Veen, *Signals and Systems*, 2nd ed., Wiley, 2005, p. 253.

[13] M. Abramowitz and I. Stegun, *Handbook of Mathematical Functions with Formulas, Graphs, and Mathematical Tables*, 1st ed. New York: Dover Publications, 1964, p. 355.

[14] C. Craeye, "A series representation for the intermediate-field transmittance between apertures," *Proc. EMTS Conf.*, Espoo, Aug. 15-18, 2016.